Time to Failure Analysis of Single Mode Long-wavelength InGaAsP Vertical-Cavity Surface-Emitting Lasers

Mohamad Ali Naeemi, Saeid Marjani*, and Ali Peiravi
Department of Electrical Engineering, Ferdowsi University of Mashhad, Mashhad, Iran
*saeid.marjani@stu-mail.um.ac.ir
51269404-فوتونیک و اپتوالکترونیک-ادوات نیمه هادی و فرآیند ساخت آن- قابلیت اطمینان

Abstract— **In this paper, we investigate the time to failure (tf) analysis of a Single Mode 1.55 µm InGaAsP vertical cavity surface emitting laser (VCSEL) with two different electrical confinement structures. The electrical confinement introduced by the oxide aperture or air-posted design are compared with conventional structure. Air-posted VCSEL shows an average of 7.43X and 19.83X Improvement in time to failure than that of the similar oxide confined and conventional VCSEL, respectively. This paper provides key results of the device characteristics, including the DC V-I, junction temperature as a function of the optical power and the time to failure vs. junction temperature. Results suggest that the 1.55 µm InGaAsP air-posted VCSEL seems to be the most optimal choice for light sources in high reliability optical communication systems.**

Keywords- Time to failure; InGaAsP; Long-wavelength; VCSEL;

I. INTRODUCTION

In recent years, the vertical cavity surface emitting lasers (VCSELs) have attracted extremely [1]. VCSEL is one of the key light sources used in high performance optical communication systems where single mode operation, high output power, high speed modulation and low manufacturing cost are necessary [2]. High optical gain in the active area, high temperature, low threshold current and high thermal conductivity in the reflecting mirrors are the main difficulties in developing VCSELs which are used in the field of optical spectroscopy [3]. When all lateral modes except one are suppressed, a fully single mode VCSEL operation is achieved. Mainly, a single lobe distribution in a desirable lateral direction defines lasing of the fundamental mode. If carriers are confined to the central part of the device, this modal distribution has best overlap with the gain's radial distribution. In a real device, the injected current has distributed over all of active region while the fundamental mode has appreciable amplitude in the center. Consequently, it is necessary to funnel the current into the center of the active region. There have been several approaches to address this issue: selective oxidation [4], proton implantation [5] or structured tunnel junction [6]. On the one hand, narrowing the current aperture causes the reduction of the emitted power and on the other hand, broadening of the current aperture favors multimode operation. Hence, it is necessary to use additional structuring of VCSELs for their single mode operation with broader current apertures. This can be assured by anti-resonant profile of the refractive index in the distributed Bragg reflectors (DBRs) [7], surface etching [8], surface grating [9] and photonic crystals (PhC) [10].

There are several reasons why the development of high-power InP-based VCSELs has not been so successful within these years as follows: 1) Need to develop a high-efficiency bottom-emitting single-device; 2) Need to improve the growth and process uniformity for cm-scale chips; 3) Need to improve the packaging for reliability and kW-level heat-removal [11]. While work on the reliability and time to failure of GaInNAs and InAlGaAs oxide confined and proton-implanted VCSELs on GaAs and InP substrates has been done [12, 13], the reliability and time to failure of InGaAsP air-posted VCSEL developed on GaAs has never been reported.

In this paper, the impact of the oxide confined (OC) and air-posted electrical confinement schemes on the time to failure of Single Mode 1.55 um InGaAsP VCSEL are investigated and compared with conventional VCSEL. The paper is organized as follows: Section II briefly describes the theoretical model and discusses the physics of failure for the VCSELs, Sec. III provides the details of the VCSEL structures, and Sec. IV presents the obtained numerical results. Finally, in Sec. V, we conclude the paper.

II. THEORY

In modeling VCSEL, we must consider the electrical, optical and thermal interaction during VCSEL performance [14]. Thus, the base of simulation is to solve Poisson and continuity equations for electrons and holes. Poisson's equation is defined by [15]:

$$\nabla \bullet (\varepsilon \nabla \Psi) = \rho \tag{1}$$

where ψ is electrostatic potential, ρ is local charge density and ε is local permittivity. The continuity equations of electron and hole are given by [15]:

$$\frac{\partial n}{\partial t} = G_n - R_n + \frac{1}{q}\nabla.\vec{J}_n \tag{2}$$

$$\frac{\partial p}{\partial t} = G_p - R_p + \frac{1}{q}\nabla.\vec{J}_p \tag{3}$$

where n and p are the electron and hole concentrations, J_n and J_p are the electron and hole current densities, G_n and G_p are the generation rates for electrons and holes, R_n and R_p are the recombination rates and q is the magnitude of electron charge.

The fundamental semiconductor equations (1)-(3) are solved self-consistently together with Helmholtz and the photon rate equations. The applied technique for solution of Helmholtz equation is based on effective frequency method [16]. Two-dimensional Helmholtz equation is solved to determine the transverse optical field profile and is given by [15]:

$$\nabla^2 E(r,z,\varphi)+\frac{\omega_0}{c^2}\varepsilon(r,z,\varphi,\omega)E(r,z,\varphi)=0 \qquad (4)$$

where ω is the frequency, ε(r, z, φ, ω) is the complex dielectric permittivity, E(r, z, φ) is the optical electric field and c is the speed of light in vacuum.

The light power equation relates electrical and optical models. The photon rate equation is given by [15]:

$$\frac{dS_m}{dt}=(\frac{c}{N_{eff}}G_m-\frac{1}{\tau_{ph_m}}-\frac{cL}{N_{eff}})S_m+R_{sp_m} \qquad (5)$$

where S_m is the photon number ,G_m is the modal gain, R_{spm} is the modal spontaneous emission rate, L represents the losses in the laser, N_{eff} is the group effective refractive index, τ_{phm} is the modal photon lifetime and c is the speed of light in vacuum. The m refers to the modal number.

The heat flow equation has the form [15]:

$$C\frac{\partial T_L}{\partial t}=\nabla(\kappa\nabla T_L)+H \qquad (6)$$

where C is the heat capacitance per unit volume, κ is the thermal conductivity, T_L is the local lattice temperature and H is the heat generation term.

The heat generation equation has the form [15]:

$$H=[\frac{\overrightarrow{|J_n|}^2}{q\mu_n n}+\frac{\overrightarrow{|J_p|}^2}{q\mu_p p}]+q(R-G)[\phi_p-\phi_n+T_L(P_p-P_n)] \qquad (7)$$
$$-T_L(\overrightarrow{J_n}\nabla P_n+\overrightarrow{J_p}\nabla P_p)$$

Where: $[\frac{\overrightarrow{|J_n|}^2}{q\mu_n n}+\frac{\overrightarrow{|J_p|}^2}{q\mu_p p}]$ is the Joule heating term, $q(R-G)[\phi_p-\phi_n+T_L(P_p-P_n)]$ is the recombination and generation heating and cooling term, $-T_L(\overrightarrow{J_n}\nabla P_n+\overrightarrow{J_p}\nabla P_p)$ accounts for the Peltier and Thomson effects.

In addition, all important, usually non-linear, interactions between the optical, electrical, thermal and recombination phenomena are also taken into account with the aid of the self-consistent iteration algorithm, including: gain-induced wave-guiding; thermal focusing; self-focusing; temperature dependence of optical gain, absorption coefficients, the energy gaps, electrical conductivities, thermal conductivities; carrier-concentration dependence of electrical

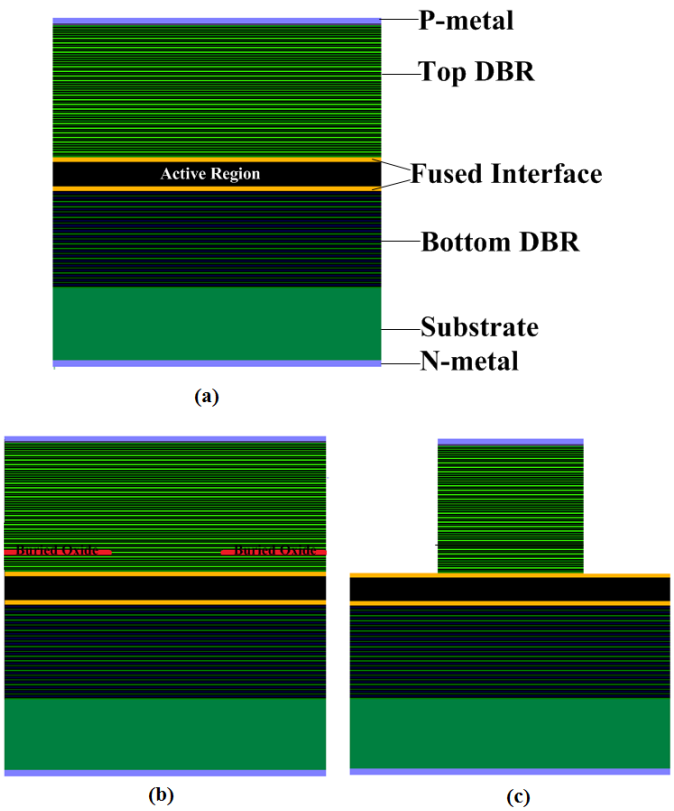

Figure 1. Schematic structure of the double-fused VCSEL analyzed: a) Conventional b) Oxide confined c) Air-posted VCSEL

Conductivities, optical gain, absorption coefficients and the energy gaps; wavelength dependences of optical gain and absorption coefficients. Eq. (1)-(7) provide an approach that can account for the mutual dependence of electrical, thermal, optical and elements of heat sources. In this paper, we employ ATLAS numerical-based simulation software to assist as in the device design and simulation [15].

III. VCSEL STRUCTURE STUDIED

The analyzed structure is similar to the one recently reported in [17-18] has been chosen as a model structure for the analysis of the 1.55 μm InGaAsP VCSEL. The active region consists of six quantum wells where the well is 5.5 nm $In_{0.76}Ga_{0.24}As_{0.82}P_{0.18}$ and the barrier is 8 nm $In_{0.48}Ga_{0.52}As_{0.82}P_{0.18}$.In both sides of this active region, there is InP and there is GaAs on the top. The top mirror is 30 layers of GaAs/$Al_{0.33}Ga_{0.67}As$ with index of refraction of 3.38 and 3.05 respectively, and the bottom mirror has 28 layers of GaAs/AlAs with index of refraction of 3.38 and 2.89, respectively (Structure A). In the OC VCSEL, the incorporation of a high aluminum content layer ($Al_{0.98}Ga_{0.02}As$) in two DBR periods above the active region allows for selective oxidation [19] as shown Fig.1 (structure B). Another confinement solution that takes advantage of the index guiding is that of air-post VCSELs as demonstrated shown Fig.1 (structure C). The layer thickness, doping, majority carrier mobility, refractive index, temperature coefficient of n, absorption coefficient, and thermal conductivity of the layers for the device simulated are listed in Table 1.

TABLE I. Parameters of the structure (l layer thickness, N_{dop} doping, μ majority carrier mobility, n refractive index, dn/dT temperature coefficient of n, α absorption coefficient, and κ thermal conductivity.)

Parameter Unit	*l* (μm)	N_{dop} ($1/cm^3$)	μ ($cm^2/V\ s$)	n	dn/dT ($10^{-4}/K$)	α (1/cm)	κ (W/cm K)
Au/Ti (Contact)	0.200	_____	_____	0.83	_____	684000	0.67
p-GaAs	0.020	2×10^{19}	_____	3.38	3	500	0.44
p-GaAs	0.182	4×10^{17}	_____	3.38	3	25	0.22
p-$Al_{0.67}Ga_{0.33}As$ (DBR)	0.127	4×10^{17}	_____	3.05	2	25	0.22
p-GaAs (DBR)	0.115	4×10^{17}	_____	3.38	3	25	0.44
p-GaAs (Spacer)	0.020	4×10^{17}	_____	3.38	3	25	0.44
p-GaAs (Spacer)	0.010	4×10^{19}	_____	3.38	3	1000	0.44
p-InP (Spacer)	0.178	1×10^{18}	30	3.17	2	24	0.68
p-Inp (Spacer)	0.100	1×10^{16}	150	3.17	2	0.24	0.68
$In_{0.76}Ga_{0.24}As_{0.82}P_{0.18}$ (QW)	0.0055	_____	100	3.6	2	54	0.043
$In_{0.48}Ga_{0.52}As_{0.82}P_{0.18}$ (Barrier)	0.008	_____	100	3.4	2	54	0.043
n-InP (Spacer)	0.258	5×10^{18}	4600	3.15	2	8	0.68
n-GaAs (Spacer)	0.050	1×10^{18}	_____	3.38	3	6	0.44
n-GaAs (DBR)	0.115	1×10^{18}	_____	3.38	3	6	0.22
n-AlAs (DBR)	0.134	1×10^{18}	_____	2.89	1	3	0.22
n-GaAs (Substrate)	450	5×10^{18}	_____	3.38	3	5.8	0.44

IV. RESULTS

The present work allows for determination of the optimum VCSEL structure that is found by comparison of the time to failure. Heat loss from the modeled VCSEL device was specified using thermal contacts at the top electrode, bottom electrode and the device sidewall. The thermal contacts define thermal conductivities to simulate heat loss from radiation via exposed surfaces or conduction through the semiconducting material to a heat-sink.

Fig.2 shows the voltage versus current curve for different structures. The DC V-I characteristics exhibit that the air-post structure has higher series resistance, which should be mainly due to etching on the top DBR and the surface recombination of carrier concentration. Due to the blocking of the current flow in the active region, oxide confined and air-post structures exhibit extremely low threshold current in comparison with the conventional structure [20].

Fig.3 shows the junction temperature as a function of the optical power. As seen, the air-post structure has a higher junction temperature at constant optical power. Due to the removal of the semiconductor surrounding the etched mesa, and the fact that the current must pass through a smaller constriction, the thermal resistance is high.

Reliability is measured through Accelerated Life Testing (ALT) that employs the widely accepted modified erying electromigration stress acceleration model. This model

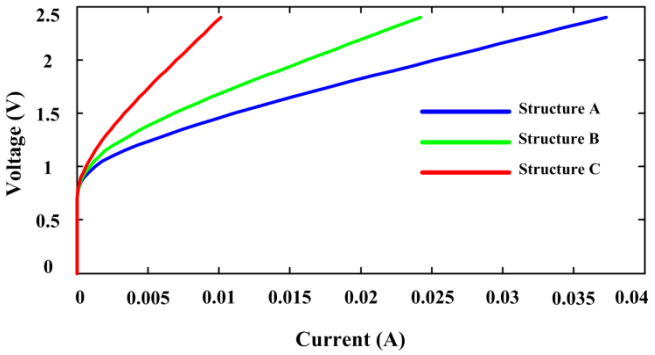

Figure 2. DC V-I characteristics for different structures.

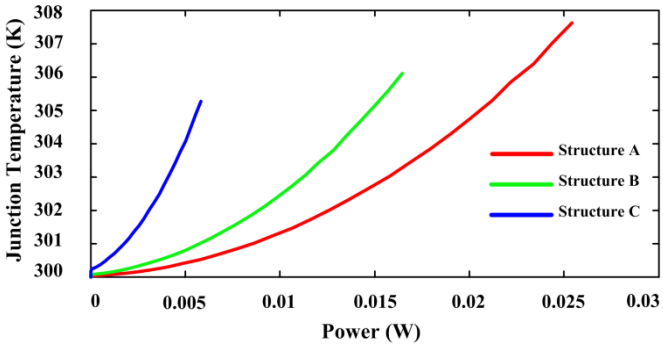

Figure 3. Junction temperature as a function of optical power.

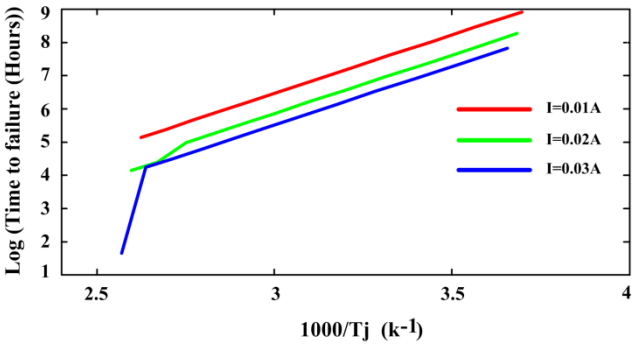

Figure 4. Logarithmic time to failure of conventional structure as a function of junction temperature for different currents.

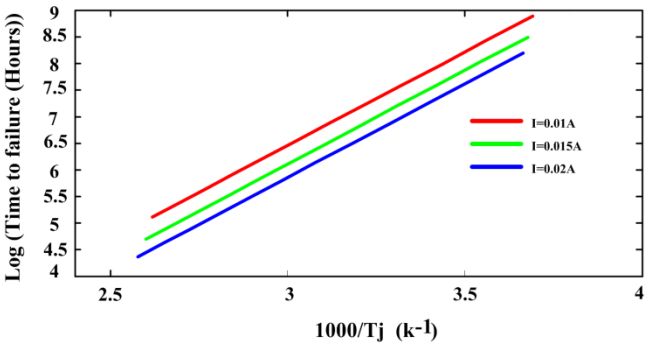

Figure 5. Logarithmic time to failure of oxide confined structure vs junction temperature for different currents.

includes current density and arrehenius temperature acceleration factors and is given by [21]:

$$tf = AJ^{-N}\exp(\frac{Ea}{K_B T}) \quad (8)$$

where tf is time to failure, A is a scaling factor, J is current density, N is current acceleration factor that is usually between 2-3 (2 in this analysis), Ea is activation energy (0.7 eV in this analysis), K_B is the boltzman's constant, and T is VCSEL junction temperature.

The time to failure of different structures as a function of junction temperature for different current at room temperature are logarithmically plotted in Figs.4-6. As can be seen, unlike some other semiconductor lasers, VCSEL degradation is linear. For comparison, Fig.7 shows the logarithmic time to failure of different structures at constant voltage. As seen, the air-post structure exhibits a remarkable improvement of time to failure of more than 7X compared to the other structures. Although this structure has a higher junction temperature, its much lower current yields this improvement. (i.e. 303.4 and 0.006 A for the air-post; and 302.5 K and 0.016 A for oxide confined VCSEL at 2 V). As seen, air-posted VCSEL shows an average of 7.43X and 19.83X improvement in time to failure compared to similar oxide confined and conventional VCSEL, respectively. Therefore, air-posted VCSEL seems to be the most optimal choice for light sources in high reliability optical communication systems.

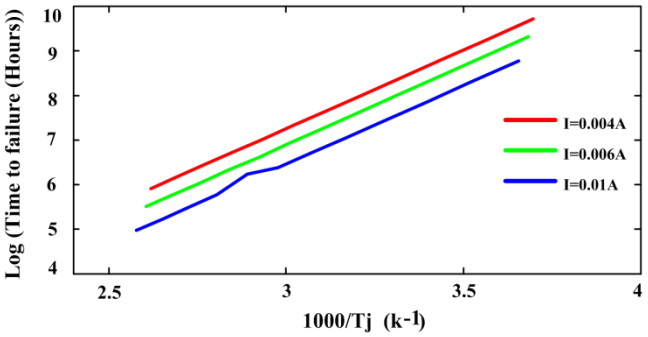

Figure 6. Logarithmic time to failure of air-posted structure as a function of junction temperature for different currents.

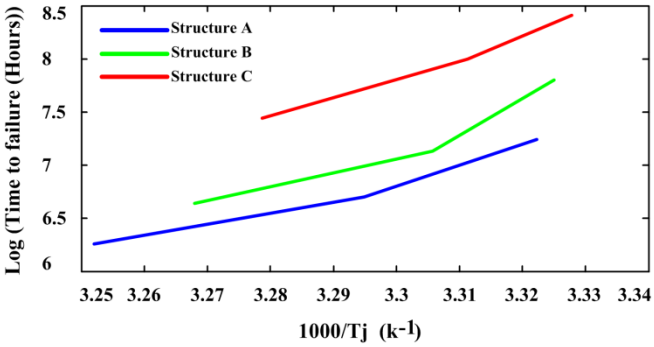

Figure 7. Comparing the logarithmic time to failure of different structures at constant voltages.

V. CONCLUSION

Time to failure of a Single Mode 1.55μm InGaAsP vertical cavity surface emitting laser with two different electrical confinement structures was analyzed and compared with conventional structure. Air-posted VCSEL shows higher time to failure than that of the similar oxide confined and conventional VCSEL. In summary, the results indicate that the air-post structure exhibit remarkable improvement in time to failure for light sources and is suitable for use in high reliability optical communication systems.

REFERENCES

[1] K. Iga, "Surface-emitting laser-its birth and generation of new optoelectronic field," J. IEEE Select. Topics Electron, vol.6, pp. 1201-1215, 2000.

[2] M. Dems, R. Kotynski, and K. Panajotov, "Plane Wave Admittance Method - a novel approach for determining the electromagnetic modes in photonic structures," J. Opt. Express, vol.13, pp. 3196-3207, 2005.

[3] E. Kapon, A. Sirbu, "Power-efficient answer," Nature Photonics vol.3, pp. 27-29, 2009.

[4] C. Jung, R. Jager, M. Grabherr, P. Schnitzer, R. Michalzik, B. Weigl, S. Muller, and K. J. Ebeling, "4.8 mW single-mode oxide confined top surface emitting vertical-cavity laser diodes," Electron. Lett., vol. 33, pp. 1790-1791, 1997.

[5] R. A. Morgan, G. D. Guth, M. W. Focht, M. T. Asom, K. Kojima, L. E. Rogers, S. E. Callis, "Transverse mode control of vertical-cavity top-surface-emitting lasers," IEEE Photon. Technol. Lett., vol. 4, pp. 374-377, 1993.

[6] E. Kapon, A. Sirbu, “Long-wavelength VCSELS Power-efficient Answer,” Nat. Photon. vol. 3 pp 27-28, 2009.
[7] D. Zhou, L. J. Mawst, “High-Power Single-Mode Anti resonant Reflecting Optical Waveguide-Type Vertical-Cavity Surface-Emitting Lasers” IEEE. J. Quantum Electron, vol. 38 pp 1599-1606, 2002.
[8] P. Debernardi, H. J. Unold, J. Maehnss, R. Michalzik, G. P. Bava, K. J. Ebeling, “Single-Mode, Single-Polarization VCSELs via Elliptical Surface Etching: Experiments and Theory” IEEE J. Sel. Top. Quantum Electron. vol. 9 pp 1394-1404, 2003.
[9] A. Haglund, J. S. Gustavsson, J. Bengtsson, P. Jedrasik, A. Larsson, “Design and Evaluation of Fundamental-Mode and Polarization-Stabilized VCSELs With a Subwavelength Surface Grating” IEEE. J. Quantum Electron, vol. 42 pp 231-240, 2006.
[10] D. F. Siriani, M. P. Tan, A. M. Kasten, A. C. Lehman Harren, P. O. Leisher, J. D. Sulkin, J. J. Raftery, Jr., A. J. Danner, A. V. Giannopoulos, K. D. Choquette, “Mode Control in Photonic Crystal Vertical-Cavity Surface-Emitting Lasers and Coherent Arrays” IEEE J. Sel. Top. Quantum Electron. vol. 15 pp 909-917, 2009.
[11] Robert W. Herrick, “Reliability of Vertical-Cavity Surface-Emitting Lasers”, Japanese Journal of Applied Physics, vol.51, pp. 11PC01, 2012.
[12] J. Jewell, et al., “Commercial GaInNAs VCSELs grown by MBE,” Phys. Stat. Solidi (c), vol. 5, no. 9, pp. 2951-2959, 2008.
[13] Alexei Sirbu, G. Suruceanu, V. Iakovlev, A. Mereuta, Z. Mickovic, A. Caliman, and E. Kapon, “Reliability of 1310 nm Wafer Fused VCSELs”, IEEE Photonics Technology Letters, vol.25, pp. 1555-1558, 2013.
[14] P. S. Menon, K. Kumarajah, M. Ismail, B. Y. M. Majlis, S. Shaari, “Long-wavelength MQW Vertical-cavity Surface Emitting Laser: Effects of Lattice Temperature”, Journal of Optical Communications. Vol 31, pp. 81-84, 2010.
[15] SILVACO International Incorporated, ATLAS User’s Manual, Version 5.12.0.R. SILVACO, Inc. , USA, 2010.
[16] Wenzel, H. Wunsche, H.-J, “The effective frequency method in the analysis of vertical-cavity surface-emitting lasers,” J. IEEE Quantum Electronics, vol.33, pp. 1156, 1997.
[17] P. Suthitha Menon, Kumarajah Kandiah, and Sahbudin Shaari, “Variation of MQW Design Parameters in a GaAs/InP-Based LW-VCSEL and its Effects on the Spectral Linewidth” J. Nonlinear Optic. Phys. Mat. Vol. 19, pp.209, 2010.
[18] P. S. Menon, K. Kumarajah, M. Ismail, B. Y. M. Majlis1, S. Shaari, “Long-wavelength MQW Vertical-cavity Surface Emitting Laser: Effects of Lattice Temperature”, J. Opt. Commun., Vol.31, pp. 081-084, 2010.
[19] R. De La Rue “Photonic Crystal Components: Harnessing the Power of the Photon” Optics and Photonics News vol. 17, pp. 30-35, 2006.
[20] R. Michalzik, VCSELs -Fundamentals, Technology and Applications of Vertical-Cavity Surface-Emitting Lasers, Springer Series in Optical Sciences, vol. 166, Berlin: Springer-Verlag, 2012.
[21] NIST/SEMATECH, e-Handbook of Statistical Methods, http://www.itl.nist.gov/div898/handbook/, 2003.